

Article

Comparative Phytotoxicity of Metallic Elements on Duckweed *Lemna gibba* L. Using Growth- and Chlorophyll Fluorescence Induction-Based Endpoints

Muhammad Irfan ¹, Ilona Mészáros ¹, Sándor Szabó ² and Viktor Oláh ^{1,*}

¹ Department of Botany, Institute of Biology and Ecology, Faculty of Science and Technology, University of Debrecen, Egyetem Square 1, H-4032 Debrecen, Hungary; muhadirfan6167@gmail.com (M.I.); immeszaros@unideb.hu (I.M.)

² Department of Biology, Institute of Environmental Sciences, University of Nyiregyhaza, H-4401 Nyiregyhaza, Hungary

* Correspondence: olahviktor@unideb.hu

Abstract: In this study, we exposed a commonly used duckweed species—*Lemna gibba* L.—to twelve environmentally relevant metals and metalloids under laboratory conditions. The phytotoxic effects were evaluated in a multi-well-plate-based experimental setup by means of the chlorophyll fluorescence imaging method. This technique allowed the simultaneous measuring of the growth and photosynthetic parameters in the same samples. The inhibition of relative growth rates (based on frond number and area) and photochemical efficiency (F_v/F_o and $Y(II)$) were both calculated from the obtained chlorophyll fluorescence images. In the applied test system, growth-inhibition-based phytotoxicity endpoints proved to be more sensitive than chlorophyll-fluorescence-based ones. Frond area growth inhibition was the most responsive parameter with a median EC_{50} of 1.75 mg L⁻¹, while F_v/F_o , the more responsive chlorophyll-fluorescence-based endpoint, resulted in a 5.34 mg L⁻¹ median EC_{50} for the tested metals. Ag (EC_{50} 0.005–1.27 mg L⁻¹), Hg (EC_{50} 0.24–4.87 mg L⁻¹) and Cu (EC_{50} 0.37–1.86 mg L⁻¹) were the most toxic elements among the tested ones, while As(V) (EC_{50} 47.15–132.18 mg L⁻¹), Cr(III) (EC_{50} 6.22–19.92 mg L⁻¹), Se(VI) (EC_{50} 1.73–10.39 mg L⁻¹) and Zn (EC_{50} 3.88–350.56 mg L⁻¹) were the least toxic ones. The results highlighted that multi-well-plate-based duckweed phytotoxicity assays may reduce space, time and sample volume requirements compared to the standard duckweed growth inhibition tests. These benefits, however, come with lowered test sensitivity. Our multi-well-plate-based test setup resulted in considerably higher median EC_{50} (3.21 mg L⁻¹) for frond-number-based growth inhibition than the 0.683 mg L⁻¹ median EC_{50} derived from corresponding data from the literature with standardized *Lemna*-tests. Under strong acute phytotoxicity, frond parts with impaired photochemical functionality may become undetectable by chlorophyll fluorometers. Consequently, the plant parts that are still detectable display a virtually higher average photosynthetic performance, leading to an underestimation of phytotoxicity. Nevertheless, multi-well-plate-based duckweed phytotoxicity assays, combined with chlorophyll fluorescence imaging, offer definite advantages in the rapid screening of large sample series or multiple species/clones. As chlorophyll fluorescence images provide information both on the photochemical performance of the test plants and their morphology, a joint analysis of the two endpoint groups is recommended in multi-well-plate-based duckweed phytotoxicity assays to maximize the information gained from the tests.

Keywords: duckweed; *Lemna gibba*; phytotoxicity; growth inhibition; chlorophyll fluorescence induction; heavy metal; metalloid



Citation: Irfan, M.; Mészáros, I.; Szabó, S.; Oláh, V. Comparative Phytotoxicity of Metallic Elements on Duckweed *Lemna gibba* L. Using Growth- and Chlorophyll Fluorescence Induction-Based Endpoints. *Plants* **2024**, *13*, 215. <https://doi.org/10.3390/plants13020215>

Academic Editor: Juan Barceló

Received: 7 December 2023

Revised: 6 January 2024

Accepted: 7 January 2024

Published: 12 January 2024



Copyright: © 2024 by the authors. Licensee MDPI, Basel, Switzerland. This article is an open access article distributed under the terms and conditions of the Creative Commons Attribution (CC BY) license (<https://creativecommons.org/licenses/by/4.0/>).

1. Introduction

Duckweeds (Lemnaceae) are recommended for ecotoxicological studies as model plants for aquatic macrophytes because of their sensitivity, simple anatomy and fast growth

rate [1,2]. Furthermore, duckweeds are also being studied as a source of biomass and biofuel production [3–6], and as phytoremediating agents [7–10]. For toxicity testing, *Lemna gibba* and *L. minor* are the recommended species in *Lemna*-tests according to the OECD guidelines [11]. In these standardized duckweed toxicity tests, the effects of environmental stressors are principally measured in terms of growth inhibition (Figure 1). Growth inhibition can be determined based on changes in frond number, area and the fresh or dry weight of the cultures, respectively [11,12]. Furthermore, toxicological studies also incorporated additional test endpoints, such as chlorophyll content [10,13,14], enzyme activities [15,16], colony size [17,18] and root length [19,20]. More recently, as an emerging non-invasive technique, the chlorophyll fluorescence (ChlF) induction method has also been increasingly utilized in various plant- and algae-based ecotoxicological studies [21–23].

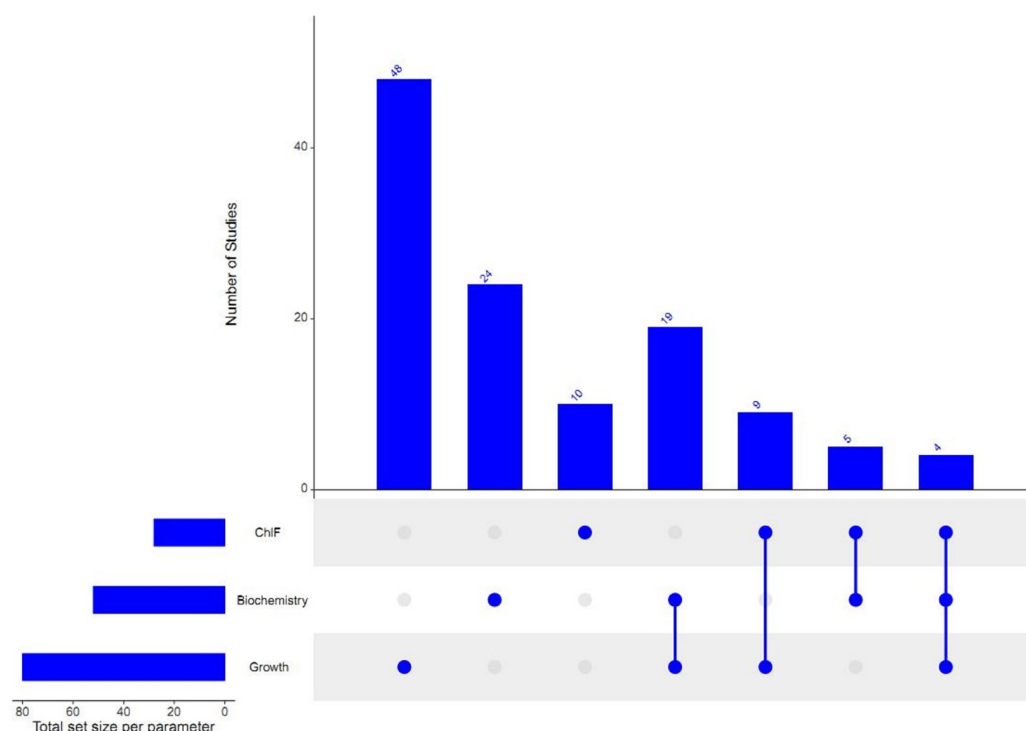


Figure 1. The occurrence of different test endpoints based on growth, biochemical markers and chlorophyll fluorescence induction parameters (ChlF) in duckweed phytotoxicity studies published between 2012 and 2023. The studied species, the parameters within the three endpoint groups and the references used are provided in the Supplementary File S1.

ChlF-based indicators are proxies for photosynthetic processes. Thus, the method offers high sensitivity in terms of both exposure duration and toxicant concentration [24]. Certain types of imaging chlorophyll fluorometers, such as the Maxi Imaging-PAM (Heinz Walz GmbH, Effeltrich, Germany) and FluorCam (Photon Systems Instruments, Brno, Czech Republic), were designed to suit phytotoxicological applications, e.g., by fitting the dimensions of multi-well plates and offering specific setting options for toxicity assays. However, the availability of a wide range of ChlF parameters, coupled with the selective application of only a few ones by different studies, makes data comparisons difficult [24]. Moreover, further research is needed to comparatively evaluate ChlF-based indicators with jointly measured growth responses [25].

The OECD duckweed toxicity tests are conducted for seven days, and use a minimum of 100 mL growth medium [11]. Large sample series or the need for rapid risk assessment, however, may challenge this standardized protocol. Recent studies have adapted duckweed tests in multi-well plates (usually 6-, 12- or 24-well plates) using a smaller volume of test medium for 3–7 days [19,24,26–28]. Such small-scale, multi-well-plate-based experiments can be managed in a limited space and with fewer resources, promising a

potential alternative to standard toxicity testing [29–31]. So far, however, most multi-well-plate-based studies with duckweeds have focused on small sets of toxicants and/or on narrow concentration ranges. Consequently, a comprehensive evaluation of the suitability and limitations of such experimental set-ups by involving a wider range of toxicants is still needed. Similarly, further research is inevitable on the broader applicability of ChlF-based endpoints in phytotoxicology [24]. In this regard, ChlF imaging is of special interest as this technique provides spatially resolved information. By bearing in mind the potential of joint morphometric and photosynthetic analyses, this method offers a high throughput multi-approach tool to study plant responses [32,33]. The interchangeability of morphometric and photosynthetic responses in the lower and higher extremes of phytotoxicity, however, is yet to be resolved. Duckweeds are particularly suitable for such comparative analyses as they easily fit into multi-well plates and their nearly two-dimensional body-plan is optimal for image analysis. To address the above questions, this study aimed to (i) provide a comprehensive phytotoxicity dataset for *L. gibba* gained in a multi-well-plate-based setup for 12 environmentally relevant metals and metalloids, and (ii) compare the responsiveness of growth-based and chlorophyll-fluorescence-based phytotoxicity endpoints to the tested elements by using the same chlorophyll fluorescence images.

2. Materials and Methods

2.1. Test Materials and Experimental Design

Axenic *Lemna gibba* L. cultures (clone #UD0101, originally isolated in E-Hungary) maintained at the Department of Botany, University of Debrecen, Hungary, were used for this study. The stock cultures were initiated with 6–8 healthy colonies, and grown in 300 mL conical flasks with 100 mL sterile modified Steinberg medium for 7 days prior to the tests [24]. A total of 12 environmentally relevant metals and metalloids (including different oxidation states) were tested in a series of at least eight nominal concentrations. The applied concentration ranges were based on pilot experiments, and the series was designed to cover approximately three magnitudes by doubling the previous concentration at every step. For Ag, Cr(VI) and Se(VI), the pilot experiments indicated highly divergent responses for different endpoints. Thus, we covered wider concentration ranges with additional treatment levels for these metals. The tested elements and concentrations were as follows: silver (AgNO_3 ; 0.76 ng L^{-1} – 0.25 mg L^{-1}), arsenite (i.e., As(III) as NaAsO_2 ; 0.078 – 10 mg L^{-1}), arsenate (i.e., As(V) as Na_2HAsO_4 ; 0.78 – 100 mg L^{-1}), cadmium (CdCl_2 ; 0.078 – 10 mg L^{-1}), chromite (i.e., Cr(III) as $\text{KCr}(\text{SO}_4)_2 \cdot 12\text{H}_2\text{O}$; 0.78 – 100 mg L^{-1}), chromate (i.e., Cr(VI) as K_2CrO_4 ; 0.0012 – 10 mg L^{-1}), copper ($\text{CuSO}_4 \cdot 5\text{H}_2\text{O}$; 0.078 – 10 mg L^{-1}), mercury (HgCl_2 ; 0.078 – 10 mg L^{-1}), nickel ($\text{NiSO}_4 \cdot 7\text{H}_2\text{O}$; 0.078 – 10 mg L^{-1}), selenite (Se(IV) as Na_2SeO_3 ; 0.078 – 10 mg L^{-1}), selenate (i.e., Se(VI) as $\text{Na}_2\text{SeO}_4 \cdot 10 \text{ H}_2\text{O}$; 0.002 – 10 mg L^{-1}) and zinc ($\text{ZnSO}_4 \cdot 7\text{H}_2\text{O}$; 0.78 – 100 mg L^{-1}). For the treatments, standard 12-well tissue culture plates were used. Each experimental series included four parallel control wells with 4–4 mL of pure Steinberg medium. The treatment wells contained 4 mL Steinberg medium spiked with the respective toxicant concentrations in quadruplicates. A single colony of 3–4 healthy fronds was transferred into each well as a starting inoculum. The test plants were then treated for three days ($72 \pm 2 \text{ h}$) under continuous white irradiation (PPFD: $60 \pm 10 \mu\text{E m}^{-2} \text{ s}^{-1}$), at a temperature of $22 \pm 2 \text{ }^\circ\text{C}$ [10]. All experiments with respect to the toxicant and concentration range were repeated twice following the same protocol and under identical ambient conditions.

2.2. In Vivo Chlorophyll Fluorescence Induction Measurements

The photosynthetic parameters were measured by means of the in vivo chlorophyll fluorescence imaging method. A Maxi Imaging-PAM chlorophyll fluorometer was used, equipped with a blue-colored LED imaging unit (with a peak intensity at 450 nm) and mounted with an IMAG-K6 digital camera (Heinz Walz GmbH, Effeltrich, Germany). The unit was operated via ImagingWin v2.47 software (Heinz Walz GmbH, Effeltrich, Germany). On the 3rd day of the experiments, we took ChlF images of plants in each

plate according to the following protocol. Firstly, the treated plants in multi-well plates were taken out from the culturing room and quickly placed into the measuring chamber of the instrument. Then, the plants were illuminated by a continuous actinic light (450 nm, $81 \mu\text{mol s}^{-1} \text{m}^{-2}$) for 60 s to maintain their light-acclimated state. After 60 s of actinic illumination, while still irradiating the plants, we measured the steady-state ChlF yield (F_s) and then applied a strong saturation light pulse ($\sim 4000 \mu\text{E m}^{-2} \text{s}^{-1}$) to determine the maximum ChlF yield (F_m'). As a second step, the plants were dark-adapted for 20 min, allowing them to reach fully oxidized state of PSII. After dark adaptation, we placed the plates back in the measuring chamber, and applied a weak, non-inductive measuring light (intensity: 2, frequency: 1) followed by a saturating pulse to measure ground (F_o) and maximum ChlF yields (F_m) in the dark-adapted plants, respectively. The basic ChlF parameters of dark-adapted and light-adapted plant samples were used for calculating the following proxies of photosynthetic efficiency averaged on a well basis [34,35]:

$$F_v/F_o = (F_m - F_o)/F_o$$

$$Y(\text{II}) = \Delta F/F_m' ; \text{ where } \Delta F = F_m' - F_s$$

F_v/F_o is an analogue of the widely used F_v/F_m —i.e., the maximal quantum yield of PSII in the dark-adapted state. This was chosen because of its higher responsiveness compared to F_v/F_m [24]. $Y(\text{II})$ is proportional to the actual quantum yield of PSII in a light-acclimated state under the applied ambient conditions [36].

2.3. Measurement of Growth Inhibition

We obtained relative growth rates (RGRs) of cultures using the chlorophyll fluorescence images exported from the ImagingWin v2.47 software (Heinz Walz GmbH, Germany). For this purpose, the F_m images of plants taken on the 0th and 3rd day of the experiments were exported to JPEG files with a 640×480 pixel resolution. ImageJ 1.54d software was used for the measurement of total area and frond number of the cultures [37]. For determining plant area, the background and roots were removed on the basis of Hue, Saturation and Brightness by means of the 'Threshold Colour' plugin [38]. Then, the filtered images were converted to binary, and the plant area in each well was calculated via the 'Analyze Particles' function. To visually count fronds, the 'cell counter' plugin was applied. We calculated the relative growth rates of cultures with respect to both the plant area (RGR_{area}) and the frond number ($\text{RGR}_{\text{frond}}$) according to the following formula [11]:

$$\text{RGR}_X = \ln(X_f - X_i)/(t_f - t_i)$$

where,

X = area or number of fronds;

X_i = initial value of the respective growth parameter;

X_f = final value of the respective growth parameter;

t_i = starting day of treatments (i.e., 0);

t_f = final day of treatments (i.e., 3).

2.4. Data Analysis and Statistics

Experimental data were pooled from the two repeated experiments with four internal parallel replicates with respect to each metal or metalloid. Thus, an overall sample size of $n = 8$ for every concentration was analyzed. In order to analyze the concentration–response relationships, three-parameter log-logistic models (LL.3) were fitted by means of the 'drc' package [39] in RStudio [40]. The suitability of the fitted models was first visually checked and then tested through the 'lack of fit' test ('modelFit' function) and 'Pseudo-R²' ('cor' function). The toxicity of metals and metalloids and the sensitivity of the analyzed test endpoints were characterized by the calculated effective concentrations (EC) resulting in a 20% (EC₂₀) and 50% (EC₅₀) inhibition of the respective endpoint. For that, the 'ED'

function of the ‘drc’ package was used. A correlation matrix (Spearman’s correlation) of the calculated effective concentrations was constructed using the ‘corrplot’ package [41] in RStudio. Pairwise comparisons (paired sample Wilcoxon signed ranks test) of the calculated effective concentrations were performed by means of OriginPro 2016 (version b9.3.226; Academic, Northampton, MA, USA).

3. Results and Discussion

3.1. Growth-Inhibition-Based Endpoints

The average doubling time for the control cultures of *L. gibba* was 1.90 ± 0.24 days in terms of frond area, fulfilling the validity requirements of the OECD [11] guidelines (<2.5 days). Similarly, in terms of frond number, a doubling time of 1.80 ± 0.22 days was recorded by the end of the 3-day-long tests. The corresponding average growth rates for frond area and frond number were 0.37 ± 0.04 and 0.39 ± 0.05 , respectively. The growth inhibitory effects of metals and metalloids in higher concentrations were clearly developed by the end of the 3 days of exposure (Figure 2, further plots for RGR_{frond} , F_v/F_0 and $Y(II)$ are provided in Figures S5–S7). Based on the calculated EC_{50} values (Supplementary Table S1), the order of phytotoxic potential of the tested elements and oxidation forms was as follows:

RGR_{frond} : Ag > Cu > Hg > Cd > As(III) > Ni > Cr(VI) > Se(IV) > Se(VI) > Cr(III) > Zn > As(V)

RGR_{area} : Ag > Hg > Cu > Cr(VI) > Cd > Se(VI) > As(III) > Ni > Zn > Se(IV) > Cr(III) > As(V)

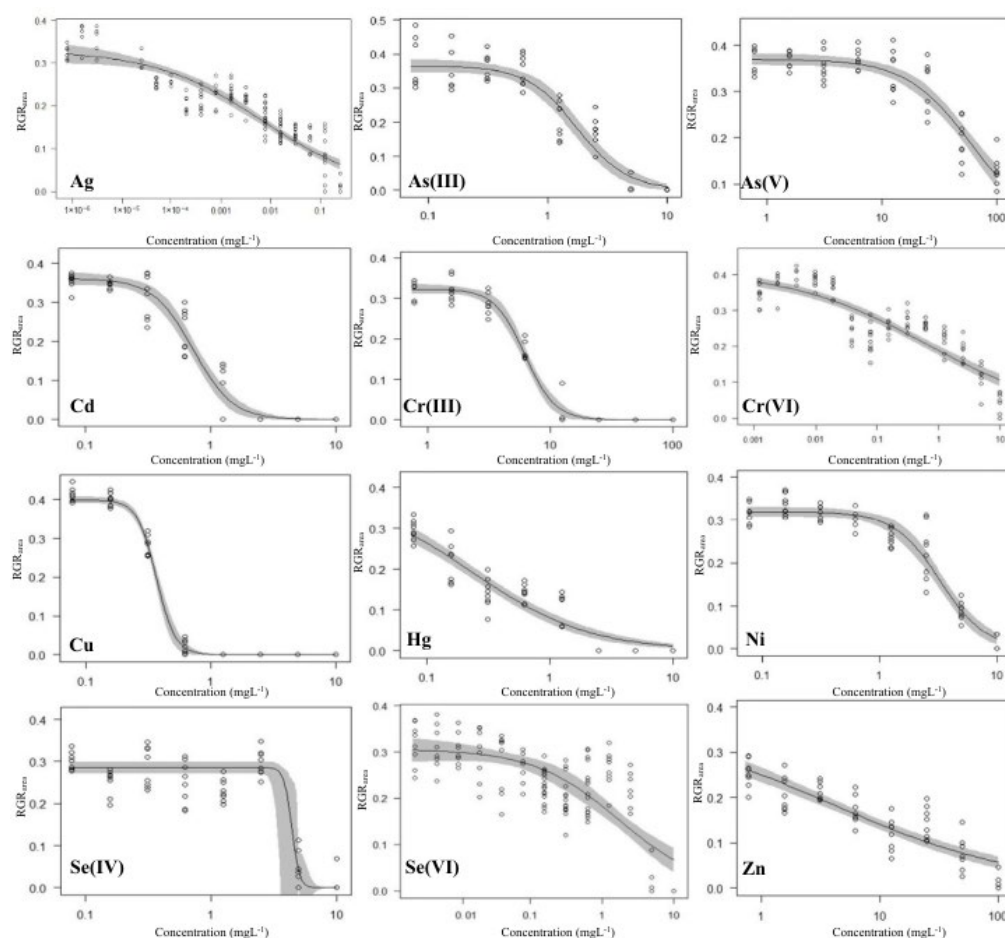


Figure 2. The 3-parameter log-logistic concentration–response model fittings of RGR_{area} for the tested metals and metalloids. Circles denote individual measurements; solid lines and shaded areas denote the fitted models and the corresponding standard errors of estimates.

The calculated effective concentrations for different metals were spread over a wide concentration range (Figure 3). In addition, the paired sample Wilcoxon signed ranks tests showed considerably higher responsivity of RGR_{area} to the applied metals and metalloids than that of RGR_{frond} , with $p < 0.001$ for both EC_{20} and EC_{50} .

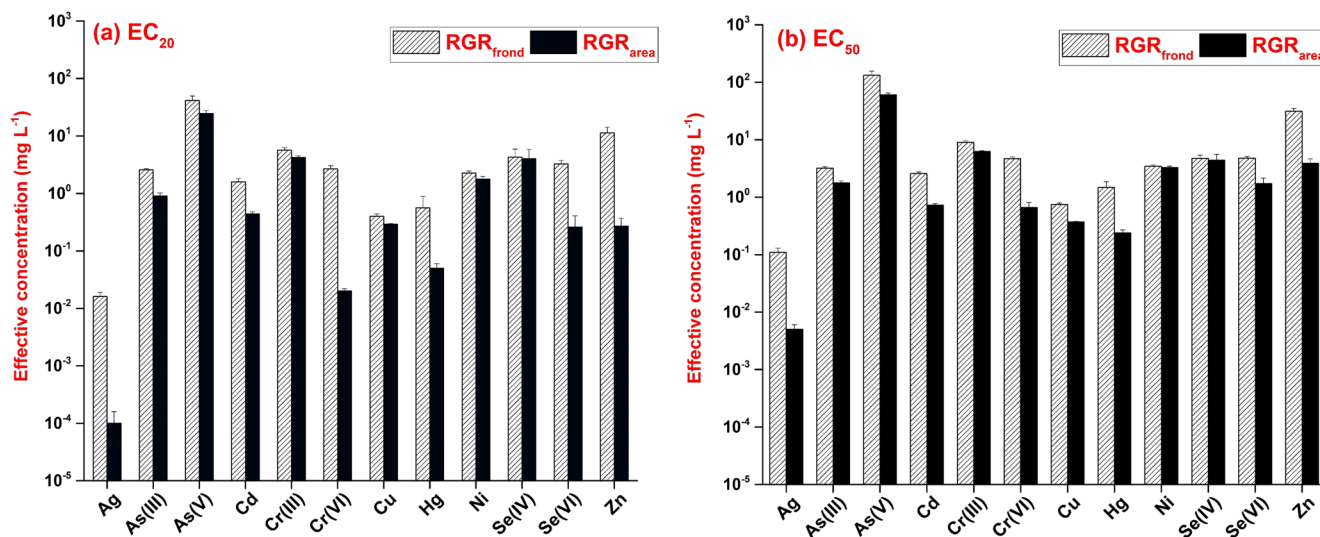


Figure 3. Effective concentrations of the 12 tested metals and metalloids resulting in (a) 20% (EC_{20}), and (b) 50% inhibition (EC_{50}) in the frond number—(RGR_{frond} , striped bars) and frond-area-based relative growth rates (RGR_{area} , black bars). The concentrations and standard errors of estimates (error bars) were calculated based on the fitted 3-parameter log-logistic models. Note the logarithmic scale of the y-axis.

Out of the 12 tested toxicants, Ag proved to be the most toxic with the lowest effective concentrations for both RGR_{area} and RGR_{frond} . Ag was associated with the induction of oxidative stress and cellular injury in *L. minor* [42]. Additional toxic effects of Ag were also observed in the form of biomass reduction, root abscission and colony disintegration in *Spirodela polyrhiza* [43]. Hg was the second most toxic element among those tested, followed by Cu and Cd (Figure 3). Hg induces oxidative damage, a reduction in the chlorophyll content, DNA damage and, ultimately, cell death [44]. Cu and Cd also affect the photosynthetic pigments and impair the antioxidant defense in duckweeds [45]. On the other extreme of the phytotoxicity spectrum, As(V) and Cr(III) resulted in the highest effective concentrations under the applied experimental conditions. As(V) did not even result in a 50% inhibition in RGR_{frond} within the applied concentration range (Supplementary Table S1 and Figure S5). Zn showed low toxicity to RGR_{frond} , while it had intermediate growth inhibition on RGR_{area} compared to other applied toxicants. The different sensitivities of the two endpoints suggested a stress-induced morphogenic response [46], where the inhibiting effect on frond production built up slower along with increasing Zn concentrations, but the newly produced fronds were smaller in size due to restricted elongation.

Our results were comparable to the previously published data in the literature. As(V) was the least toxic based on growth inhibition (i.e., frond number, fresh weight, dry weight) and photosynthetic pigment contents in a previous comparative study on *L. minor* exposed to ten heavy metals [47]. The effective concentrations for RGR_{frond} in *L. gibba* were comparable to the respective values in *L. minor* for Ag, As(III) and Cu [47,48]. Zn was also found to be moderately toxic to duckweeds, up to 10 mg L⁻¹ in previous reports [49,50]. The EC_{50} values for Cu from our multi-well-plate-based experiments were also comparable to those ones reported by Khellaf and Zerdaoui [51] using the standard OECD protocol with *L. gibba*. In terms of the 9 commonly analyzed metals, however, our data for *L. gibba* indicated lower sensitivity compared to the previously reported data for *L. minor*

by Naumann et al. [47] in ISO [12] standard tests (Table 1). The results for *L. gibba* (current study) and *L. minor* [47] showed a weak correlation for EC₂₀ (Spearman's $\rho = 0.55$, $p = 0.125$), while the calculated EC₅₀ data correlated more strongly (Spearman's $\rho = 0.78$, $p = 0.012$). Similarly, the RGR_{frond} and RGR_{area} EC₅₀ values in the present study were considerably higher when compared to those previously obtained in our lab using the OECD [11] protocol. Those earlier experiments were performed with *S. polyrhiza* (UD0401 clone) and provided several times lower EC₅₀ for RGR_{area} in treatments with Ni and Cr(VI) (0.184 and 0.188 mg L⁻¹ [52]), Cd (0.104 mg L⁻¹ [18]), Hg (0.137 mg L⁻¹ [53]) and As(III) and As(V) (1.33 and 25.04 mg L⁻¹, Hepp et al., unpublished data). Ni also proved to be three–four times less toxic in our multi-well-plate-based setup with *L. gibba* compared to data reported for the same species following the OECD protocol [51]. Besides species-specific metal tolerance, these differences were most probably due to the shorter exposure duration and lower dose (i.e., toxicant-to-biomass ratio) in our setup.

Table 1. Comparison of the sensitivity in the multi-well-plate-based setup (current study) with previously reported effective concentrations obtained from ISO-standard [12] tests by Naumann et al. [47]. The paired sample Wilcoxon signed ranks tests were performed on the calculated 20% (EC₂₀) and 50% (EC₅₀) effective concentrations for RGR_{frond} using the following 9 common metals in the two studies: Ag, As(III), As(V), Cd, Cr(VI), Cu, Hg, Ni and Zn.

Median Effective Concentration (RGR _{frond})				
	Current Study (<i>L. gibba</i>)	Naumann et al. [47] (<i>L. minor</i>)	W	<i>p</i>
EC ₂₀	2.27	0.086	2	0.023
EC ₅₀	3.21	0.683	3	0.020

In agreement with previous studies, the frond-area-based growth rate showed greater sensitivity to metal-induced inhibition than the frond-number-based one [54,55]. This fact can be explained by the different nature of the two growth parameters. Frond area is a continuous measure while frond number is a quantile one. Daughter fronds may develop to smaller sizes under stress and contribute proportionally less to the total frond area than to the frond number in cultures. This results in stronger growth inhibition, with lower EC values for the former parameter. Additionally, in standard duckweed tests, photos for area measurements are usually taken in the visible spectral range, and can include both healthy and chlorotic spots into the measured frond area. ChlF images, on the other hand, show only the photosynthetically active areas of fronds, while chlorotic regions with a weak ChlF signal can remain undetected. This way, the observed area can drop considerably even when frond number stays seemingly high. Hence, ChlF-based area measurement might have also contributed to the different sensitivities of the two growth rates.

3.2. Chlorophyll-Fluorescence-Induction-Based Endpoints

For the two analyzed ChlF-based endpoints, the respective EC₅₀ values (Table S5) indicated the following order of phytotoxicity amongst the tested metals and metalloids:

F_v/F_o: Cr(VI) > Cu > Ag > As(III) > Cd > Hg > Ni > Se(IV) > Se(VI) > Cr(III) > Zn > As(V)

Y(II): Ag > Cr(VI) > Cu > As(III) > Cd > Hg > Ni > Se(VI) > Se(IV) > Cr(III) > As(V) > Zn

The paired sample Wilcoxon signed ranks test confirmed that the calculated EC₂₀ for the two ChlF parameters did not differ significantly (medians: 2.665 and 3.21 mg L⁻¹ for F_v/F_o and for Y(II), respectively, $p = 0.176$). However, the EC₅₀ values indicated a significantly higher sensitivity of F_v/F_o to the tested metals and metalloids (medians: 5.34 and 5.755 mg L⁻¹ for F_v/F_o and Y(II), respectively, $p = 0.021$). Y(II) was more responsive to Ag, Hg and Se(VI), but F_v/F_o resulted in lower EC values for the rest of the tested metals (Figure 4). For Ag, Se(VI) and Zn, however, we could only calculate the

extrapolated effective concentrations, which exceeded the applied concentration ranges (Supplementary Table S1). In that regard, Ag was so toxic to *L. gibba* that the plants lost their viability even before reaching 20% inhibition in either ChlF parameter. For Zn, on the other hand, we could only calculate an unrealistically high ($\sim 350 \text{ mg L}^{-1}$) EC_{50} in case of Y(II) due to this extrapolation. Contrastingly, EC_{50} for F_v/F_o stayed in the applied concentration range. For Se(VI), the extrapolated EC_{50} for F_v/F_o was only slightly above the applied concentration range.

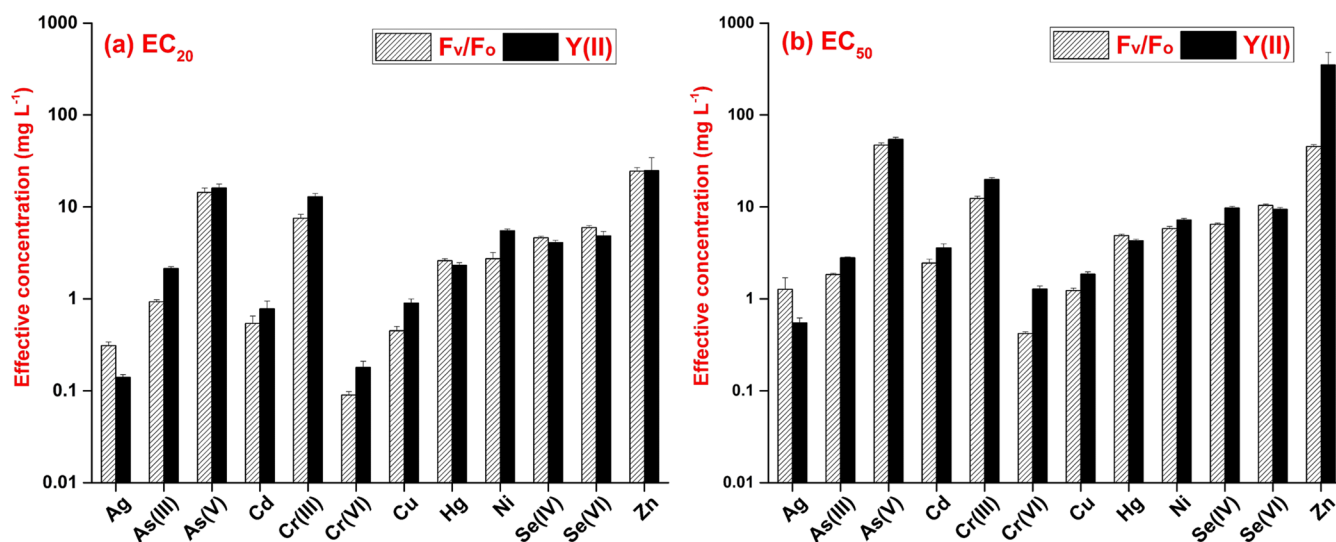


Figure 4. Effective concentrations of the 12 tested metals and metalloids resulting in (a) 20% (EC_{20}), and (b) 50% inhibition (EC_{50}) in F_v/F_o (striped bars) and Y(II) (black bars). The concentrations and standard errors of estimates (error bars) were calculated based on the fitted 3-parameter log-logistic models. Note the logarithmic scale of the y-axis.

When we compared the more sensitive growth-based endpoint (RGR_{area}) to the more sensitive ChlF-based one (F_v/F_o), the paired sample Wilcoxon signed ranks test confirmed a significantly higher responsivity of growth to metals and metalloids. The difference was seven-fold in the case of the calculated EC_{20} values (medians: 0.365 and 2.665 mg L^{-1} for RGR_{area} and F_v/F_o , respectively, $p = 0.042$) and three-fold for the calculated EC_{50} values (medians: 1.75 and 5.34 mg L^{-1} for RGR_{area} and F_v/F_o , respectively, $p = 0.042$). As an exception, F_v/F_o proved to be more sensitive than RGR_{area} in the case of As(V) and Cr(VI). We also observed that the comparability of the two parameters mainly decreased in the case of extremely high or low toxicity (e.g., Ag, Se(VI) and Zn). The reason for such diverging responses might be that the higher the toxicant concentration, the greater the loss of apparent frond area due to chlorotic regions. Thus, using ChlF-based F_m images for measuring growth inhibition might result in overestimation. As a limitation of the ChlF imaging method in duckweed phytotoxicity tests, a threshold was set for the images at a minimal fluorescence level in order to reduce background noise [56]. In some cases, further pixels of severely impacted frond parts were also non-detectable under the saturating light pulse. As a result, only those frond regions that were still detectable were considered for calculating F_v/F_o and Y(II). Thus, a virtually higher functionality of photochemical efficiency was maintained due to excluding the most affected frond parts (Figure 5).

A common stress response in duckweeds is the premature detachment of fronds from the parent colony [57]. In our study, this separation was observed in the presence of highly toxic elements (e.g., Ag and Hg) and under the highest concentration treatments. Most of the prematurely separated fronds did not produce further daughter fronds, thus reducing the overall relative growth rate. Nevertheless, these separated small-sized fronds still maintained a certain degree of photosynthetic activity (Figure 5). Combined with the

above-described bias by chlorotic spots, these results point to the importance of cautious interpretation of ChlF-based endpoints in duckweed tests.

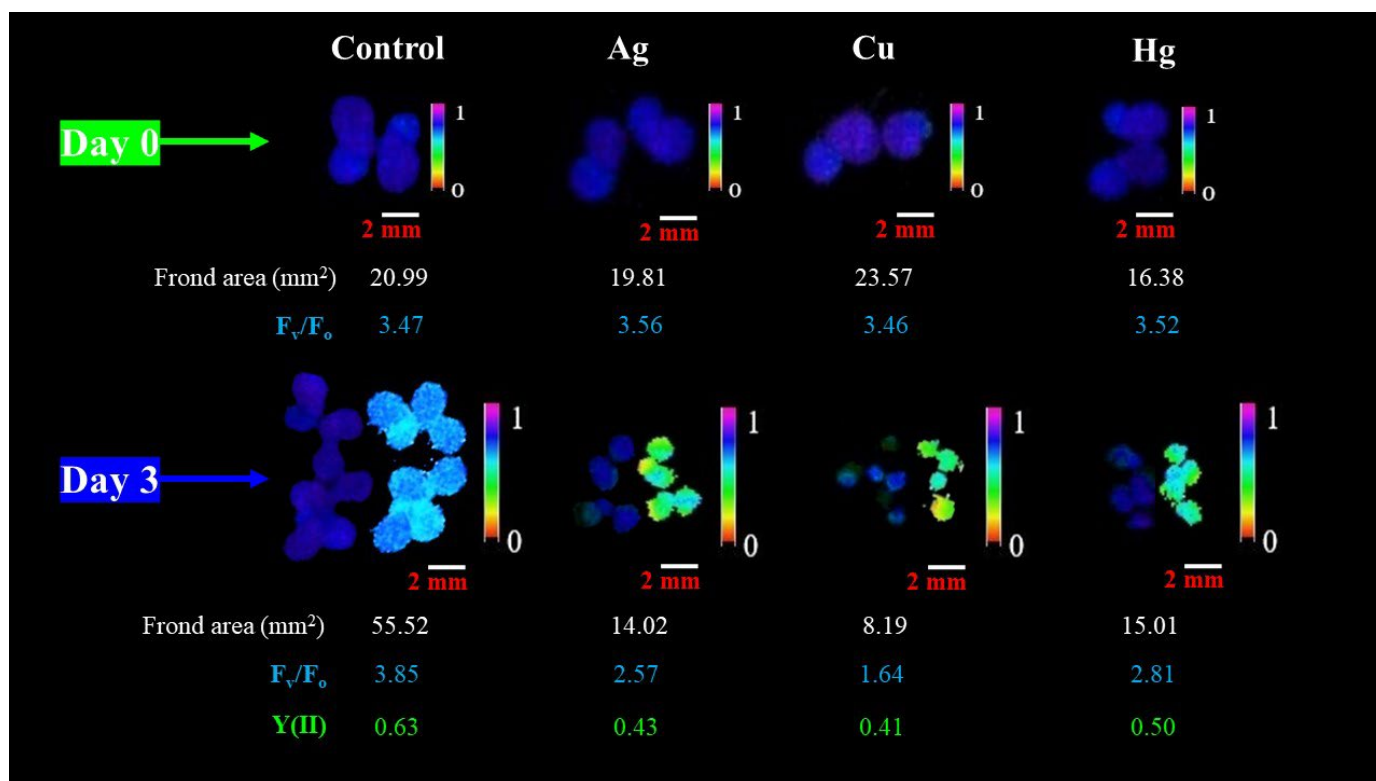


Figure 5. Chlorophyll fluorescence images of the same control and treated *L. gibba* colonies at the beginning (day 0) and final day (day 3) of tests. The treated plants showed significant loss in the detectable frond area due to chlorosis, while the residual, photosynthetically active frond parts still maintained >50% of control F_v/F_o and Y(II). Ag, Cu and Hg denote treatments with $3.125 \mu\text{g L}^{-1}$ Ag, 1.25 mg L^{-1} Cu and 2.5 mg L^{-1} Hg, respectively. The upper row shows F_v/F_m while the lower row represents F_v/F_m (left side) and Y(II) (right side) for the respective treatments.

Even if growth- and ChlF-based endpoints showed diverging sensitivities in the higher and lower extremes of phytotoxicity, their overall correlation indicated strong interdependence (Figure 6). In this regard, our results were consistent with previous data from the literature reporting that a decline in Y(II) strongly correlated with growth inhibition in duckweeds treated with common PSII inhibitor herbicides (e.g., atrazine and diuron) [58]. Similarly, ChlF-derived endpoints proved to be very sensitive in *L. minor* in response to Cu toxicity [59] and also correlated well with changes in fresh weight under bisphenol A exposure [60]. When the applied toxicants (perfluorooctanoic acid and dimethyl phthalate) did not result in growth inhibition, however, ChlF-based endpoints were also unresponsive [33,61]. Our results thus highlight that ChlF-based endpoints can characterize phytotoxicity with certain limitations. More importantly, this non-invasive method can provide functional insight into the modes of action behind toxic effects. Since chlorophyll fluorescence images bear the possibility of extracting information on both the morphology (i.e., growth) and the functional state (i.e., photosynthesis), the joint measurement of both endpoint groups is recommended in duckweed phytotoxicity assays to maximize the information gained from the tests.

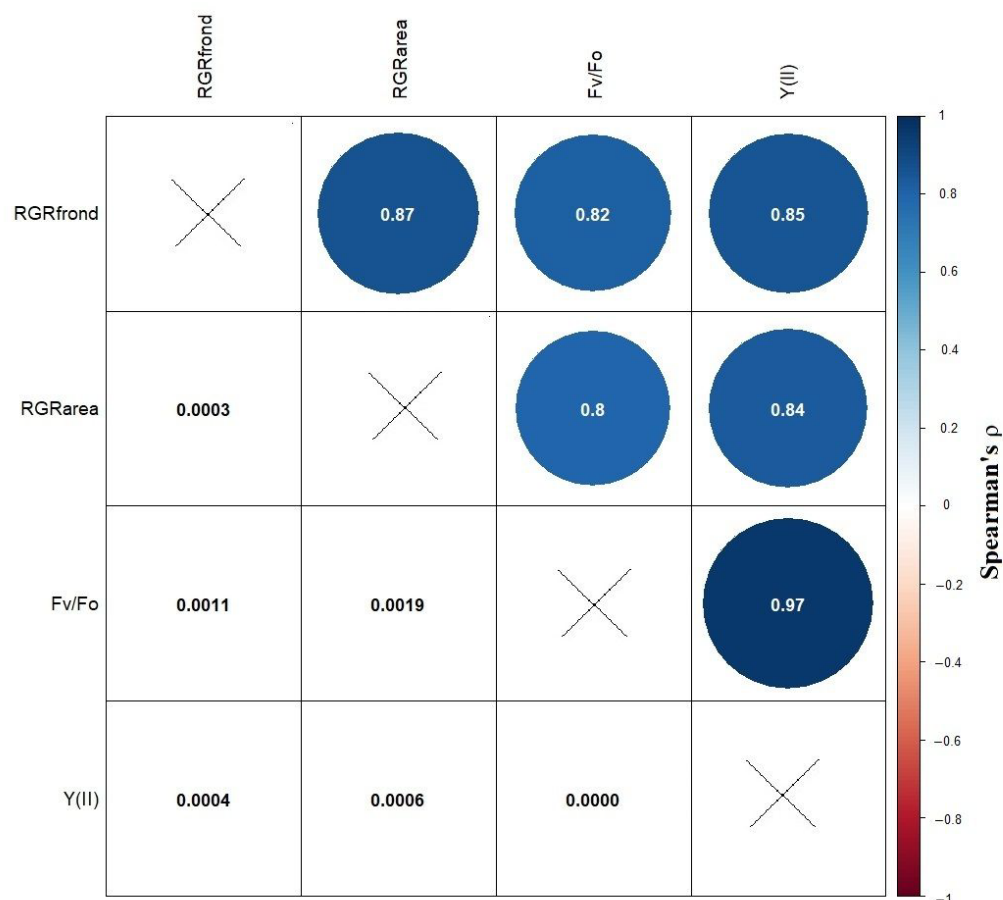


Figure 6. Correlation matrix based on Spearman's ρ (upper triangle) and the corresponding p -values (lower triangle) for the calculated EC_{50} values for the growth- and ChlF-based endpoints.

4. Conclusions

Our results revealed that small-scale, multi-well-plate-based phytotoxicity tests with duckweeds offer definite advantages by reducing space, time and sample volume requirements, but at the expense of lower sensitivity. The order of phytotoxic potential amongst the tested elements was comparable to previous studies using OECD and ISO standard duckweed tests, but the calculated effective concentrations were higher than those in the standardized tests. In addition, when comparing the calculated effective concentrations, we found noticeable differences in the responsivity of the tested endpoints. The results pointed out that chlorophyll-fluorescence-induction-based phytotoxicity endpoints—at least in the case of duckweeds—cannot fully replace the growth-inhibition-based ones. The method inevitably underestimates the photosynthesis-inhibiting effects under strong acute phytotoxicity due to the exclusion of chlorotic frond parts. Nevertheless, chlorophyll fluorescence imaging is valuable in providing a non-invasive tool to jointly analyze duckweed growth and photosynthetic responses in phytotoxicity tests. Thus, the application of multi-well-plate-based duckweed phytotoxicity assays, combined with chlorophyll fluorescence imaging, can facilitate the screening of large sample series or multiple duckweed species/clones.

Supplementary Materials: The following supporting information can be downloaded at <https://www.mdpi.com/article/10.3390/plants13020215/s1>, File S1: metadata for Figures S1–S4 (main text); Figure S5: 3-parameter log-logistic concentration–response model fittings of RGR_{frond} ; Figure S6: 3-parameter log-logistic concentration–response model fittings of F_v/F_o ; Figure S7: 3-parameter log-logistic concentration–response model fittings of $Y(II)$; and Table S1: The results of the 3-

parameter log-logistic model fittings with calculated EC₂₀ and EC₅₀ values for the studied endpoints. References [62–111] are cited in the supplementary materials.

Author Contributions: Conceptualization, V.O.; methodology, V.O., M.I. and I.M.; formal analysis, M.I.; investigation, M.I.; writing—original draft preparation, M.I.; writing—review and editing, M.I., V.O., I.M. and S.S.; visualization, M.I. and V.O.; supervision, V.O.; project administration, V.O.; funding acquisition, V.O. All authors have read and agreed to the published version of the manuscript.

Funding: This research was funded by the National Research, Development and Innovation Office — NKFIH— of the Hungarian Ministry for Innovation and Technology, grant number OTKA FK 134296.

Data Availability Statement: The datasets used in the present study are available from the corresponding author on reasonable request.

Acknowledgments: The authors are grateful to the Agora Science Centre (Debrecen, Hungary) for providing the opportunity to use the Imaging-PAM instrument. Viktor Oláh was supported by the János Bolyai Research Scholarship of the Hungarian Academy of Sciences and by the ÚNKP-23-5 New National Excellence Program of the Ministry for Culture and Innovation, sourced from the National Research, Development and Innovation Fund. Sándor Szabó was financed by the Scientific Board of the University of Nyíregyháza. Muhammad Irfan is thankful for the support of the Tempus Public Foundation (Hungary) within the framework of the Stipendium Hungaricum Scholarship Programme.

Conflicts of Interest: The authors declare no conflicts of interest.

References

1. Radić, S.; Stipančič, D.; Cvjetko, P.; Marijanović Rajčić, M.; Širac, S.; Pevalak-Kozlina, B.; Pavlica, M. Duckweed *Lemna minor* as a Tool for Testing Toxicity and Genotoxicity of Surface Waters. *Ecotoxicol. Environ. Saf.* **2011**, *74*, 182–187. [CrossRef]
2. Yahaya, N.; Hamdan, N.H.; Zabidi, A.R.; Mohamad, A.M.; Suhaimi, M.L.H.; Johari, M.A.A.M.; Yahya, H.N.; Yahya, H. Duckweed as a Future Food: Evidence from Metabolite Profile, Nutritional and Microbial Analyses. *Future Foods* **2022**, *5*, 100128. [CrossRef]
3. Chen, G.; Zhao, K.; Li, W.; Yan, B.; Yu, Y.; Li, J.; Zhang, Y.; Xia, S.; Cheng, Z.; Lin, F.; et al. A Review on Bioenergy Production from Duckweed. *Biomass Bioenergy* **2022**, *161*, 106468. [CrossRef]
4. Cui, W.; Cheng, J.J.; Cui, C.W. Growing Duckweed for Biofuel Production: A Review. *Plant Biol.* **2015**, *17*, 16–23. [CrossRef] [PubMed]
5. Paolacci, S.; Stejskal, V.; Toner, D.; Jansen, M.A.K. Wastewater Valorisation in an Integrated Multitrophic Aquaculture System; Assessing Nutrient Removal and Biomass Production by Duckweed Species. *Environ. Pollut.* **2022**, *302*, 119059. [CrossRef] [PubMed]
6. Petersen, F.; Demann, J.; Restemeyer, D.; Olfs, H.-W.; Westendarp, H.; Appenroth, K.-J.; Ulbrich, A. Influence of Light Intensity and Spectrum on Duckweed Growth and Proteins in a Small-Scale, Re-Circulating Indoor Vertical Farm. *Plants* **2022**, *11*, 1010. [CrossRef] [PubMed]
7. Chen, G.; Fang, Y.; Huang, J.; Zhao, Y.; Li, Q.; Lai, F.; Xu, Y.; Tian, X.; He, K.; Jin, Y.; et al. Duckweed Systems for Eutrophic Water Purification through Converting Wastewater Nutrients to High-Starch Biomass: Comparative Evaluation of Three Different Genera (*Spirodela polyrrhiza*, *Lemna minor* and *Landoltia punctata*) in Monoculture or Polyculture. *RSC Adv.* **2018**, *8*, 17927–17937. [CrossRef]
8. Golob, A.; Vogel-Mikuš, K.; Brudar, N.; Germ, M. Duckweed (*Lemna minor* L.) Successfully Accumulates Selenium from Selenium-Impacted Water. *Sustainability* **2021**, *13*, 13423. [CrossRef]
9. Iqbal, J.; Javed, A.; Baig, M.A. Growth and Nutrient Removal Efficiency of Duckweed (*Lemna minor*) from Synthetic and Dumpsite Leachate under Artificial and Natural Conditions. *PLoS ONE* **2019**, *14*, e0221755. [CrossRef]
10. Szabó, S.; Zavanyi, G.; Koleszár, G.; del Castillo, D.; Oláh, V.; Braun, M. Phytoremediation, Recovery and Toxic Effects of Ionic Gadolinium Using the Free-Floating Plant *Lemna gibba*. *J. Hazard. Mater.* **2023**, *458*, 131930. [CrossRef]
11. OECD Guidelines for the Testing of Chemicals, Revised Proposal for a New Guideline 221, *Lemna* sp. Growth Inhibition Test. 2006. Available online: https://www.oecd-ilibrary.org/environment/test-no-221-lemna-sp-growth-inhibition-test_9789264016194-en (accessed on 14 September 2023).
12. ISO 20079:2005; ISO Water Quality—Determination of the Toxic Effect of Water Constituents and Waste Water on Duckweed (*Lemna minor*)—Duckweed Growth Inhibition Test. ISO: Geneva, Switzerland, 2005.
13. Yang, J.; Li, G.; Xia, M.; Chen, Y.; Chen, Y.; Kumar, S.; Sun, Z.; Li, X.; Zhao, X.; Hou, H. Combined Effects of Temperature and Nutrients on the Toxicity of Cadmium in Duckweed (*Lemna aequinoctialis*). *J. Hazard. Mater.* **2022**, *432*, 128646. [CrossRef] [PubMed]
14. Zhao, Z.; Shi, H.; Duan, D.; Li, H.; Lei, T.; Wang, M.; Zhao, H.; Zhao, Y. The Influence of Duckweed Species Diversity on Ecophysiological Tolerance to Copper Exposure. *Aquat. Toxicol.* **2015**, *164*, 92–98. [CrossRef] [PubMed]

15. Forni, C.; Braglia, R.; Harren, F.J.M.; Cristescu, S.M. Stress Responses of Duckweed (*Lemna minor* L.) and Water Velvet (*Azolla filiculoides* Lam.) to Anionic Surfactant Sodium-Dodecyl-Sulphate (SDS). *Aquat. Toxicol.* **2012**, *110–111*, 107–113. [[CrossRef](#)] [[PubMed](#)]
16. Obermeier, M.; Schröder, C.A.; Helmreich, B.; Schröder, P. The Enzymatic and Antioxidative Stress Response of *Lemna minor* to Copper and a Chloroacetamide Herbicide. *Environ. Sci. Pollut. Res. Int.* **2015**, *22*, 18495–18507. [[CrossRef](#)] [[PubMed](#)]
17. Henke, R.; Eberius, M.; Appenroth, K.-J. Induction of Frond Abscission by Metals and Other Toxic Compounds in *Lemna minor*. *Aquat. Toxicol.* **2011**, *101*, 261–265. [[CrossRef](#)] [[PubMed](#)]
18. Oláh, V.; Hepp, A.; Mészáros, I. Assessment of Giant Duckweed (*Spirodela polyrhiza* L. Schleiden) Turions as Model Objects in Ecotoxicological Applications. *Bull. Environ. Contam. Toxicol.* **2016**, *96*, 596–601. [[CrossRef](#)] [[PubMed](#)]
19. Lee, H.; De Saeger, J.; Bae, S.; Kim, M.; Depuydt, S.; Heynderickx, P.M.; Wu, D.; Han, T.; Park, J. Giant Duckweed (*Spirodela polyrhiza*) Root Growth as a Simple and Sensitive Indicator of Copper and Chromium Contamination. *Toxics* **2023**, *11*, 788. [[CrossRef](#)]
20. Zhang, L.M.; Jin, Y.; Yao, S.M.; Lei, N.F.; Chen, J.S.; Zhang, Q.; Yu, F.H. Growth and Morphological Responses of Duckweed to Clonal Fragmentation, Nutrient Availability, and Population Density. *Front. Plant Sci.* **2020**, *11*, 618. [[CrossRef](#)]
21. Chen, M.; Yin, G.; Zhao, N.; Gan, T.; Feng, C.; Gu, M.; Qi, P.; Ding, Z. Rapid and Sensitive Detection of Water Toxicity Based on Photosynthetic Inhibition Effect. *Toxics* **2021**, *9*, 321. [[CrossRef](#)]
22. Gan, T.; Yin, G.; Zhao, N.; Tan, X.; Wang, Y. A Sensitive Response Index Selection for Rapid Assessment of Heavy Metals Toxicity to the Photosynthesis of *Chlorella pyrenoidosa* Based on Rapid Chlorophyll Fluorescence Induction Kinetics. *Toxics* **2023**, *11*, 468. [[CrossRef](#)]
23. Moustaka, J.; Moustakas, M. Early-Stage Detection of Biotic and Abiotic Stress on Plants by Chlorophyll Fluorescence Imaging Analysis. *Biosensors* **2023**, *13*, 796. [[CrossRef](#)] [[PubMed](#)]
24. Oláh, V.; Hepp, A.; Irfan, M.; Mészáros, I. Chlorophyll Fluorescence Imaging-Based Duckweed Phenotyping to Assess Acute Phytotoxic Effects. *Plants* **2021**, *10*, 2763. [[CrossRef](#)] [[PubMed](#)]
25. Lee, H.; Depuydt, S.; Shin, K.; Choi, S.; Kim, G.; Lee, Y.H.; Park, J.T.; Han, T.; Park, J. Assessment of Various Toxicity Endpoints in Duckweed (*Lemna minor*) at the Physiological, Biochemical, and Molecular Levels as a Measure of Diuron Stress. *Biology* **2021**, *10*, 684. [[CrossRef](#)] [[PubMed](#)]
26. O'Brien, A.M.; Laurich, J.; Lash, E.; Frederickson, M.E. Mutualistic Outcomes Across Plant Populations, Microbes, and Environments in the Duckweed *Lemna minor*. *Microb. Ecol.* **2020**, *80*, 384–397. [[CrossRef](#)] [[PubMed](#)]
27. Zhang, Y.; Hu, Y.; Yang, B.; Ma, F.; Lu, P.; Li, L.; Wan, C.; Rayner, S.; Chen, S. Duckweed (*Lemna minor*) as a Model Plant System for the Study of Human Microbial Pathogenesis. *PLoS ONE* **2010**, *5*, e13527. [[CrossRef](#)] [[PubMed](#)]
28. De Cesare, F.; Pietrini, F.; Zacchini, M.; Scarascia Mugnozza, G.; Macagnano, A. Catechol-Loading Nanofibrous Membranes for Eco-Friendly Iron Nutrition of Plants. *Nanomaterials* **2019**, *9*, 1315. [[CrossRef](#)] [[PubMed](#)]
29. Baudo, R.; Foudoulakis, M.; Arapis, G.; Perdaen, K.; Lanneau, W.; Paxinou, A.-C.; Kouvdou, S.; Persoone, G. History and Sensitivity Comparison of the *Spirodela polyrhiza* Microbiotest and *Lemna* Toxicity Tests. *Knowl. Manag. Aquat. Ecosyst.* **2015**, *416*, 23. [[CrossRef](#)]
30. Kalčíková, G.; Marolt, G.; Kokalj, A.J.; Gotvajn, A.Ž. The Use of Multiwell Culture Plates in the Duckweed Toxicity Test—A Case Study on Zn Nanoparticles. *New Biotechnol.* **2018**, *47*, 67–72. [[CrossRef](#)]
31. Kose, T.; Lins, T.F.; Wang, J.; O'Brien, A.M.; Sinton, D.; Frederickson, M.E. Accelerated High-Throughput Imaging and Phenotyping System for Small Organisms. *PLoS ONE* **2023**, *18*, e0287739. [[CrossRef](#)]
32. Pietrini, F.; Zacchini, M. A New Ecotoxicity Assay for Aquatic Plants: Eco-Tox Photosystem Tool (ETPT). *Trends Plant Sci.* **2020**, *25*, 1266–1267. [[CrossRef](#)]
33. Pietrini, F.; Passatore, L.; Fischetti, E.; Carloni, S.; Ferrario, C.; Polesello, S.; Zacchini, M. Evaluation of Morpho-Physiological Traits and Contaminant Accumulation Ability in *Lemna minor* L. Treated with Increasing Perfluorooctanoic Acid (PFOA) Concentrations under Laboratory Conditions. *Sci. Total Environ.* **2019**, *695*, 133828. [[CrossRef](#)] [[PubMed](#)]
34. Roháček, K. Chlorophyll Fluorescence Parameters: The Definitions, Photosynthetic Meaning, and Mutual Relationships. *Photosynthetica* **2002**, *40*, 13–29. [[CrossRef](#)]
35. Mallakin, A.; Babu, T.S.; Dixon, D.G.; Greenberg, B.M. Sites of Toxicity of Specific Photooxidation Products of Anthracene to Higher Plants: Inhibition of Photosynthetic Activity and Electron Transport in *Lemna gibba* L. G-3 (Duckweed). *Environ. Toxicol.* **2002**, *17*, 462–471. [[CrossRef](#)]
36. Klughammer, C.; Schreiber, U. Complementary PS II Quantum Yields Calculated from Simple Fluorescence Parameters Measured by PAM Fluorometry and the Saturation Pulse Method. *PAM Appl. Notes* **2008**, *1*, 201–247.
37. Schneider, C.A.; Rasband, W.S.; Eliceiri, K.W. NIH Image to ImageJ: 25 Years of Image Analysis. *Nat. Methods* **2012**, *9*, 671–675. [[CrossRef](#)]
38. Landini, G. Novel Context-Based Segmentation Algorithms for Intelligent Microscopy. 2020. Available online: <https://blog.bham.ac.uk/intellimic/g-landini-software/> (accessed on 14 September 2023).
39. Ritz, C.; Baty, F.; Streibig, J.C.; Gerhard, D. Dose-Response Analysis Using R. *PLoS ONE* **2015**, *10*, e0146021. [[CrossRef](#)] [[PubMed](#)]
40. RStudio Team. *RStudio Team RStudio Desktop IDE (Version 2023.06.0-421) [Computer Software]*; PBC: Boston, MA, USA, 2023; Available online: <http://www.rstudio.com/> (accessed on 14 September 2023).

41. Wei, T.; Simko, V.R. Package ‘Corrplot’: Visualization of a Correlation Matrix (Version 0.90). 2021. Available online: <https://github.com/taiyun/corrplot> (accessed on 14 September 2023).
42. Li, H.; Mo, F.; Li, Y.; Wang, M.; Li, Z.; Hu, H.; Deng, W.; Zhang, R. Effects of Silver(I) Toxicity on Microstructure, Biochemical Activities, and Genic Material of *Lemna minor* L. with Special Reference to Application of Bioindicator. *Environ. Sci. Pollut. Res.* **2020**, *27*, 22735–22748. [[CrossRef](#)]
43. Jiang, H.-S.; Li, M.; Chang, F.-Y.; Li, W.; Yin, L.-Y. Physiological Analysis of Silver Nanoparticles and AgNO₃ Toxicity to *Spirodela polyrrhiza*. *Environ. Toxicol. Chem.* **2012**, *31*, 1880–1886. [[CrossRef](#)]
44. Zhang, T.; Lu, Q.; Su, C.; Yang, Y.; Hu, D.; Xu, Q. Mercury Induced Oxidative Stress, DNA Damage, and Activation of Antioxidative System and Hsp70 Induction in Duckweed (*Lemna minor*). *Ecotoxicol. Environ. Saf.* **2017**, *143*, 46–56. [[CrossRef](#)]
45. Hou, W.; Chen, X.; Song, G.; Wang, Q.; Chi Chang, C. Effects of Copper and Cadmium on Heavy Metal Polluted Waterbody Restoration by Duckweed (*Lemna minor*). *Plant Physiol. Biochem.* **2007**, *45*, 62–69. [[CrossRef](#)]
46. Potters, G.; Pasternak, T.P.; Guisez, Y.; Palme, K.J.; Jansen, M.A.K. Stress-Induced Morphogenic Responses: Growing out of Trouble? *Trends Plant Sci.* **2007**, *12*, 98–105. [[CrossRef](#)] [[PubMed](#)]
47. Naumann, B.; Eberius, M.; Appenroth, K.J. Growth Rate Based Dose-Response Relationships and EC-Values of Ten Heavy Metals Using the Duckweed Growth Inhibition Test (ISO 20079) with *Lemna minor* L. Clone St. *J. Plant Physiol.* **2007**, *164*, 1656–1664. [[CrossRef](#)]
48. Khellaf, N.; Zerdaoui, M. Growth Response of the Duckweed *Lemna minor* to Heavy Metal Pollution. *J. Environ. Health Sci. Eng.* **2009**, *6*, 161–166.
49. Lahive, E.; O’Callaghan, M.J.A.; Jansen, M.A.K.; O’Halloran, J. Uptake and Partitioning of Zinc in Lemnaceae. *Ecotoxicol. Lond. Engl.* **2011**, *20*, 1992–2002. [[CrossRef](#)] [[PubMed](#)]
50. Lanthemann, L.; van Moorsel, S.J. Species Interactions in Three Lemnaceae Species Growing along a Gradient of Zinc Pollution. *Ecol. Evol.* **2022**, *12*, e8646. [[CrossRef](#)] [[PubMed](#)]
51. Khellaf, N.; Zerdaoui, M. Growth Response of the Duckweed *Lemna Gibba* L. to Copper and Nickel Phytoaccumulation. *Ecotoxicology* **2010**, *19*, 1363–1368. [[CrossRef](#)] [[PubMed](#)]
52. Oláh, V.; Hepp, A.; Mészáros, I. Comparative Study on the Sensitivity of Turions and Active Fronds of Giant Duckweed (*Spirodela polyrrhiza* (L.) Schleiden) to Heavy Metal Treatments. *Chemosphere* **2015**, *132*, 40–46. [[CrossRef](#)]
53. Hepp, A.; Vaca, N.Y.G.; Kovács, F.; Tamás, M.; Oláh, V.; Mészáros, I. Effects of Hg on Growth of Active and Resting (Turions) Fronds of Giant Duckweed (*Spirodela polyrrhiza* (L.) Schleiden). In *Proceedings of the XII. Environmental Scientific Conference of the Carpathian Basin, Berehove, Ukraine, 1–4 June 2016*; Kiss, I., Pincehelyi, Z.É., Eds.; PTE TTK Szentágotthai János Protestant College: Pécs, Hungary, 2016; Volume 126, pp. 94–103, ISBN 9789634290506.
54. Markovic, M.; Neale, P.A.; Nidumolu, B.; Kumar, A. Combined Toxicity of Therapeutic Pharmaceuticals to Duckweed, *Lemna minor*. *Ecotoxicol. Environ. Saf.* **2021**, *208*, 111428. [[CrossRef](#)]
55. Oláh, V.; Hepp, A.; Gaibor Vaca, N.Y.; Tamás, M.; Mészáros, I. Retrospective Analyses of Archive Phytotoxicity Test Data Can Help in Assessing Internal Dynamics and Stability of Growth in Laboratory Duckweed Cultures. *Aquat. Toxicol.* **2018**, *201*, 40–46. [[CrossRef](#)]
56. Heinz Walz GmbH. *IMAGING-PAM M-Series Chlorophyll Fluorometer: Instrument Description and Information for Users*, 5th ed.; Heinz Walz GmbH: Effeltrich, Germany, 2019.
57. Ziegler, P.; Appenroth, K.J.; Sree, K.S. Survival Strategies of Duckweeds, the World’s Smallest Angiosperms. *Plants* **2023**, *12*, 2215. [[CrossRef](#)]
58. Park, J.; Brown, M.T.; Depuydt, S.; Kim, J.K.; Won, D.-S.; Han, T. Comparing the Acute Sensitivity of Growth and Photosynthetic Endpoints in Three *Lemna* Species Exposed to Four Herbicides. *Environ. Pollut.* **2017**, *220*, 818–827. [[CrossRef](#)]
59. Singh, H.; Kumar, D.; Soni, V. Performance of Chlorophyll a Fluorescence Parameters in *Lemna minor* under Heavy Metal Stress Induced by Various Concentration of Copper. *Sci. Rep.* **2022**, *12*, 10620. [[CrossRef](#)]
60. Liang, J.; Li, Y.; Xie, P.; Liu, C.; Yu, L.; Ma, X. Dualistic Effects of Bisphenol A on Growth, Photosynthetic and Oxidative Stress of Duckweed (*Lemna minor*). *Environ. Sci. Pollut. Res. Int.* **2022**, *29*, 87717–87729. [[CrossRef](#)]
61. Pietrini, F.; Passatore, L.; Carloni, S.; Zacchini, M. Non-Standard Physiological Endpoints to Evaluate the Toxicity of Emerging Contaminants in Aquatic Plants: A Case Study on the Exposure of *Lemna minor* L. and *Spirodela polyrrhiza* (L.) Schleid. to Dimethyl Phthalate (DMP). In *Emerging Contaminants and Plants: Interactions, Adaptations and Remediation Technologies*; Emerging Contaminants and Associated Treatment Technologies; Aftab, T., Ed.; Springer International Publishing: Cham, Switzerland, 2023; pp. 87–108, ISBN 978-3-031-22269-6.
62. Rodrigues, S.; Pinto, I.; Martins, F.; Formigo, N.; Antunes, S.C. An Ecotoxicological Approach Can Complement the Assessment of Natural Waters from Portuguese Reservoirs? *Environ. Sci. Pollut. Res. Int.* **2022**, *29*, 52147–52161. [[CrossRef](#)] [[PubMed](#)]
63. Diogo, B.S.; Rodrigues, S.; Lage, O.M.; Antunes, S.C. Are the Ecotoxicological Tools Viable to Evaluate the Effectiveness of Wastewater Treatment Plant Effluents? *Int. J. Environ. Sci. Technol.* **2023**, *20*, 11943–11962. [[CrossRef](#)]
64. Fekete-Kertész, I.; Kunglné-Nagy, Z.; Gruiz, K.; Magyar, Á.; Farkas, É.; Molnár, M. Assessing Toxicity of Organic Aquatic Micropollutants Based on the Total Chlorophyll Content of *Lemna minor* as a Sensitive Endpoint. *Period. Polytech. Chem. Eng.* **2015**, *59*, 262–271. [[CrossRef](#)]
65. Boros, B.-V.; Dascalu, D.; Ostafe, V.; Isvoran, A. Assessment of the Effects of Chitosan, Chitooligosaccharides and Their Derivatives on *Lemna minor*. *Molecules* **2022**, *27*, 6123. [[CrossRef](#)]

66. Gavina, A.; Antunes, S.C.; Pinto, G.; Claro, M.T.; Santos, C.; Gonçalves, F.; Pereira, R. Can Physiological Endpoints Improve the Sensitivity of Assays with Plants in the Risk Assessment of Contaminated Soils? *PLoS ONE* **2013**, *8*, e59748. [[CrossRef](#)]
67. Song, L.; Vijver, M.G.; Peijnenburg, W.J.G.M. Comparative Toxicity of Copper Nanoparticles across Three Lemnaceae Species. *Sci. Total Environ.* **2015**, *518–519*, 217–224. [[CrossRef](#)] [[PubMed](#)]
68. Dalton, R.L.; Nussbaumer, C.; Pick, F.R.; Boutin, C. Comparing the Sensitivity of Geographically Distinct *Lemna minor* Populations to Atrazine. *Ecotoxicol. Lond. Engl.* **2013**, *22*, 718–730. [[CrossRef](#)]
69. Kurnia, K.A.; Lin, Y.-T.; Farhan, A.; Malhotra, N.; Luong, C.T.; Hung, C.-H.; Roldan, M.J.M.; Tsao, C.-C.; Cheng, T.-S.; Hsiao, C.-D. Deep Learning-Based Automatic Duckweed Counting Using StarDist and Its Application on Measuring Growth Inhibition Potential of Rare Earth Elements as Contaminants of Emerging Concerns. *Toxics* **2023**, *11*, 680. [[CrossRef](#)] [[PubMed](#)]
70. Van Antro, M.; Prelovsek, S.; Ivanovic, S.; Gawehns, F.; Wagemaker, N.C.A.M.; Mysara, M.; Horemans, N.; Vergeer, P.; Verhoeven, K.J.F. DNA Methylation in Clonal Duckweed (*Lemna minor* L.) Lineages Reflects Current and Historical Environmental Exposures. *Mol. Ecol.* **2023**, *32*, 428–443. [[CrossRef](#)] [[PubMed](#)]
71. Roubeau Dumont, E.; Larue, C.; Lorber, S.; Gryta, H.; Billoir, E.; Gross, E.M.; Elger, A. Does Intraspecific Variability Matter in Ecological Risk Assessment? Investigation of Genotypic Variations in Three Macrophyte Species Exposed to Copper. *Aquat. Toxicol.* **2019**, *211*, 29–37. [[CrossRef](#)] [[PubMed](#)]
72. Fekete-Kertész, I.; Stirling, T.; Vaszita, E.; Berkl, Z.; Farkas, É.; Hedwig, S.; Remmen, K.; Lenz, M.; Molnár, M.; Feigl, V. Ecotoxicity Attenuation by Acid-Resistant Nanofiltration in Scandium Recovery from TiO₂ Production Waste. *Heliyon* **2023**, *9*, e15512. [[CrossRef](#)] [[PubMed](#)]
73. Andreani, T.; Nogueira, V.; Gavina, A.; Fernandes, S.; Rodrigues, J.L.; Pinto, V.V.; Ferreira, M.J.; Silva, A.M.; Pereira, C.M.; Pereira, R. Ecotoxicity to Freshwater Organisms and Cytotoxicity of Nanomaterials: Are We Generating Sufficient Data for Their Risk Assessment? *Nanomaterials* **2021**, *11*, 66. [[CrossRef](#)] [[PubMed](#)]
74. Pietrini, F.; Iannilli, V.; Passatore, L.; Carloni, S.; Sciacca, G.; Cerasa, M.; Zacchini, M. Ecotoxicological and Genotoxic Effects of Dimethyl Phthalate (DMP) on *Lemna Minor* L. and *Spirodela polyrhiza* (L.) Schleid. Plants under a Short-Term Laboratory Assay. *Sci. Total Environ.* **2022**, *806*, 150972. [[CrossRef](#)] [[PubMed](#)]
75. Groth, V.A.; Carvalho-Pereira, T.; da Silva, E.M.; Niemeyer, J.C. Ecotoxicological Assessment of Biosolids by Microcosms. *Chemosphere* **2016**, *161*, 342–348. [[CrossRef](#)]
76. Sackey, L.N.A.; Mocová, K.A.; Kočí, V. Ecotoxicological Effect of Aged Wood Leachates to Aquatic Organisms. *Water* **2020**, *12*, 2091. [[CrossRef](#)]
77. Godoy, A.A.; Kummrow, F.; Pamplin, P.A.Z. Ecotoxicological Evaluation of Propranolol Hydrochloride and Losartan Potassium to *Lemna minor* L. (1753) Individually and in Binary Mixtures. *Ecotoxicology* **2015**, *24*, 1112–1123. [[CrossRef](#)]
78. Soares, C.; Fernandes, B.; Paiva, C.; Nogueira, V.; Cachada, A.; Fidalgo, F.; Pereira, R. Ecotoxicological Relevance of Glyphosate and Flazasulfuron to Soil Habitat and Retention Functions—Single vs Combined Exposures. *J. Hazard. Mater.* **2023**, *442*, 130128. [[CrossRef](#)]
79. Ikebe Otomo, J.; Araujo de Jesus, T.; Gomes Coelho, L.H.; Rebelo Monteiro, L.; Hunter, C.; Helwig, K.; Roberts, J.; Pahl, O. Effect of Eight Common Brazilian Drugs on *Lemna minor* and *Salvinia auriculata* Growth. *Environ. Sci. Pollut. Res. Int.* **2021**, *28*, 43747–43762. [[CrossRef](#)]
80. Hlavkova, D.; Caloudova, H.; Palikova, P.; Kopel, P.; Plhalova, L.; Beklova, M.; Havelkova, B. Effect of Gold Nanoparticles and Ions Exposure on the Aquatic Organisms. *Bull. Environ. Contam. Toxicol.* **2020**, *105*, 530–537. [[CrossRef](#)] [[PubMed](#)]
81. Alkimin, G.D.; Daniel, D.; Dionísio, R.; Soares, A.M.V.M.; Barata, C.; Nunes, B. Effects of Diclofenac and Salicylic Acid Exposure on *Lemna minor*: Is Time a Factor? *Environ. Res.* **2019**, *177*, 108609. [[CrossRef](#)] [[PubMed](#)]
82. Castro, V.L.; Jonsson, C.M.; Silva, M.S.G.M.; Castanha, R.; Vallim, J.H.; da Silva, L.A.G.; de Oliveira, R.M.D.; Correa, D.S.; Ferreira, M.D. Estimates of AgNP Toxicity Thresholds in Support of Environmental Safety Policies. *J. Nanoparticle Res.* **2022**, *24*, 9. [[CrossRef](#)]
83. Alkimin, G.D.; Soares, A.M.V.M.; Barata, C.; Nunes, B. Evaluation of Ketoprofen Toxicity in Two Freshwater Species: Effects on Biochemical, Physiological and Population Endpoints. *Environ. Pollut.* **2020**, *265*, 114993. [[CrossRef](#)]
84. Alkimin, G.D.; Daniel, D.; Frankenbach, S.; Seródio, J.; Soares, A.M.V.M.; Barata, C.; Nunes, B. Evaluation of Pharmaceutical Toxic Effects of Non-Standard Endpoints on the Macrophyte Species *Lemna minor* and *Lemna gibba*. *Sci. Total Environ.* **2019**, *657*, 926–937. [[CrossRef](#)] [[PubMed](#)]
85. Castro, A.M.; Nogueira, V.; Lopes, I.; Rocha-Santos, T.; Pereira, R. Evaluation of the Potential Toxicity of Effluents from the Textile Industry before and after Treatment. *Appl. Sci.* **2019**, *9*, 3804. [[CrossRef](#)]
86. Knežević, V.; Tunić, T.; Gajić, P.; Marjan, P.; Savić, D.; Tenji, D.; Teodorović, I. Getting More Ecologically Relevant Information from Laboratory Tests: Recovery of *Lemna minor* After Exposure to Herbicides and Their Mixtures. *Arch. Environ. Contam. Toxicol.* **2016**, *71*, 572–588. [[CrossRef](#)] [[PubMed](#)]
87. Mohr, S.; Schott, J.; Hoenemann, L.; Feibicke, M. *Glyceria maxima* as New Test Species for the EU Risk Assessment for Herbicides: A Microcosm Study. *Ecotoxicol. Lond. Engl.* **2015**, *24*, 309–320. [[CrossRef](#)]
88. Magahud, J.C.; Dalumpines, S.L.P. Growth of Duckweeds (*Lemna minor* L.) as Affected by Light Intensity, Nutrient Solution Concentration, and Light × Nutrient Interaction. *Philipp. Sci. Lett.* **2021**, *14*, 119–129.

89. Burns, M.; Hanson, M.L.; Prosser, R.S.; Crossan, A.N.; Kennedy, I.R. Growth Recovery of *Lemna gibba* and *Lemna minor* Following a 7-Day Exposure to the Herbicide Diuron. *Bull. Environ. Contam. Toxicol.* **2015**, *95*, 150–156. [[CrossRef](#)]
90. Havelkova, B.; Hlavkova, D.; Kovacova, V.; Beklova, M. Herbicides in the Cave Environment: Ecotoxicological Risks. *Fresenius Environ. Bull.* **2019**, *28*, 781–786.
91. Xie, L.; Gomes, T.; Solhaug, K.A.; Song, Y.; Tollefsen, K.E. Linking Mode of Action of the Model Respiratory and Photosynthesis Uncoupler 3,5-Dichlorophenol to Adverse Outcomes in *Lemna minor*. *Aquat. Toxicol. Amst. Neth.* **2018**, *197*, 98–108. [[CrossRef](#)] [[PubMed](#)]
92. Rozman, U.; Jemec Kokalj, A.; Dolar, A.; Drobne, D.; Kalčíková, G. Long-Term Interactions between Microplastics and Floating Macrophyte *Lemna minor*: The Potential for Phytoremediation of Microplastics in the Aquatic Environment. *Sci. Total Environ.* **2022**, *831*, 154866. [[CrossRef](#)] [[PubMed](#)]
93. Tofan, L.; Niță, V.; Nenciu, M.; Coatu, V.; Lazăr, L.; Damir, N.; Vasile, D.; Popoviciu, D.R.; Brotea, A.-G.; Curtean-Bănăduc, A.M.; et al. Multiple Assays on Non-Target Organisms to Determine the Risk of Acute Environmental Toxicity in Tebuconazole-Based Fungicides Widely Used in the Black Sea Coastal Area. *Toxics* **2023**, *11*, 597. [[CrossRef](#)]
94. Varga, M.; Horvatic, J.; Barišić, L.; Lončarić, Z.; Dutour Sikirić, M.; Erceg, I.; Kočić, A.; Štolfa Čamagajevac, I. Physiological and Biochemical Effect of Silver on the Aquatic Plant *Lemna gibba* L.: Evaluation of Commercially Available Product Containing Colloidal Silver. *Aquat. Toxicol. Amst. Neth.* **2019**, *207*, 52–62. [[CrossRef](#)] [[PubMed](#)]
95. de Alkimin, G.D.; Paisio, C.; Agostini, E.; Nunes, B. Phytoremediation Processes of Domestic and Textile Effluents: Evaluation of the Efficacy and Toxicological Effects in *Lemna minor* and *Daphnia magna*. *Environ. Sci. Pollut. Res. Int.* **2020**, *27*, 4423–4441. [[CrossRef](#)] [[PubMed](#)]
96. Logeshwaran, P.; Sivaram, A.K.; Yadav, M.; Chadalavada, S.; Naidu, R.; Megharaj, M. Phytotoxicity of Class B Aqueous Firefighting Formulations, Tridol S 3 and 6% to *Lemna minor*. *Environ. Technol. Innov.* **2020**, *18*, 100688. [[CrossRef](#)]
97. Pereira, S.P.P.; Jesus, F.; Aguiar, S.; de Oliveira, R.; Fernandes, M.; Ranville, J.; Nogueira, A.J.A. Phytotoxicity of Silver Nanoparticles to *Lemna minor*: Surface Coating and Exposure Period-Related Effects. *Sci. Total Environ.* **2018**, *618*, 1389–1399. [[CrossRef](#)]
98. Mohiley, A.; Franzaring, J.; Calvo, O.C.; Fangmeier, A. Potential Toxic Effects of Aircraft De-Icers and Wastewater Samples Containing These Compounds. *Environ. Sci. Pollut. Res. Int.* **2015**, *22*, 13094–13101. [[CrossRef](#)]
99. Di Baccio, D.; Pietrini, F.; Bertolotto, P.; Pérez, S.; Barcelò, D.; Zacchini, M.; Donati, E. Response of *Lemna gibba* L. to High and Environmentally Relevant Concentrations of Ibuprofen: Removal, Metabolism and Morpho-Physiological Traits for Biomonitoring of Emerging Contaminants. *Sci. Total Environ.* **2017**, *584–585*, 363–373. [[CrossRef](#)] [[PubMed](#)]
100. Gopalapillai, Y.; Vigneault, B.; Hale, B.A. Root Length of Aquatic Plant, *Lemna minor* L., as an Optimal Toxicity Endpoint for Biomonitoring of Mining Effluents. *Integr. Environ. Assess. Manag.* **2014**, *10*, 493–497. [[CrossRef](#)]
101. Daniel, D.; de Alkimin, G.D.; Nunes, B. Single and Combined Effects of the Drugs Salicylic Acid and Acetazolamide: Adverse Changes in Physiological Parameters of the Freshwater Macrophyte, *Lemna gibba*. *Environ. Toxicol. Pharmacol.* **2020**, *79*, 103431. [[CrossRef](#)]
102. Gabriel, A.; Venâncio, C.; Sousa, J.P.; Leston, S.; Ramos, F.; Soares, A.M.V.M.; Lopes, I. Soil pH Matters in the Ecotoxicity of Basamid@to Freshwater Microalgae and Macrophytes. *Sci. Total Environ.* **2023**, *859*, 160165. [[CrossRef](#)] [[PubMed](#)]
103. Grenni, P.; Patrolecco, L.; Rauseo, J.; Spataro, F.; Di Lenola, M.; Aimola, G.; Zacchini, M.; Pietrini, F.; Di Baccio, D.; Stanton, I.C.; et al. Sulfamethoxazole Persistence in a River Water Ecosystem and Its Effects on the Natural Microbial Community and *Lemna minor* Plant. *Microchem. J.* **2019**, *149*, 103999. [[CrossRef](#)]
104. Sikorski, L.; Baciak, M.; Beš, A.; Adomas, B. The Effects of Glyphosate-Based Herbicide Formulations on *Lemna minor*, a Non-Target Species. *Aquat. Toxicol. Amst. Neth.* **2019**, *209*, 70–80. [[CrossRef](#)] [[PubMed](#)]
105. Modlitbová, P.; Hlaváček, A.; Švestková, T.; Pořízka, P.; Šimoníková, L.; Novotný, K.; Kaiser, J. The Effects of Photon-Upconversion Nanoparticles on the Growth of Radish and Duckweed: Bioaccumulation, Imaging, and Spectroscopic Studies. *Chemosphere* **2019**, *225*, 723–734. [[CrossRef](#)]
106. Kokalj, A.J.; Novak, S.; Talaber, I.; Kononenko, V.; Mali, L.B.; Vodovnik, M.; Žegura, B.; Eleršek, T.; Kalčíkova, G.; Gotvajn, A.Ž.; et al. The First Comprehensive Safety Study of Magnéli Phase Titanium Suboxides Reveals No Acute Environmental Hazard. *Environ. Sci. Nano* **2019**, *6*, 1131–1139. [[CrossRef](#)]
107. Mihajlović, V.; Tomić, T.; Tubić, A.; Molnar Jazić, J.; Ivančev Tumbas, I.; Šunjka, D.; Lazić, S.; Teodorović, I. The Impact of Humic Acid on Toxicity of Individual Herbicides and Their Mixtures to Aquatic Macrophytes. *Environ. Sci. Pollut. Res. Int.* **2019**, *26*, 23571–23582. [[CrossRef](#)]
108. Facin, F.; de Melo, J.V.S.; Lalau, C.M.; Nogueira, D.J.; Puerari, R.C.; Matias, W.G. Toxicological Effects of Leachate Extracts from Asphalt Mixtures Nanomodified under *Daphnia magna* and *Landoltia punctata* Test Organisms. *Chemosphere* **2021**, *285*, 131463. [[CrossRef](#)]
109. Xie, L.; Song, Y.; Petersen, K.; Solhaug, K.A.; Lind, O.C.; Brede, D.A.; Salbu, B.; Tollefsen, K.E. Ultraviolet B Modulates Gamma Radiation-Induced Stress Responses in *Lemna minor* at Multiple Levels of Biological Organisation. *Sci. Total Environ.* **2022**, *846*, 157457. [[CrossRef](#)]

110. Roubeau Dumont, E.; Gao, X.; Zheng, J.; Macairan, J.; Hernandez, L.M.; Baesu, A.; Bayen, S.; Robinson, S.A.; Ghoshal, S.; Tufenkji, N. Unraveling the Toxicity of Tire Wear Contamination in Three Freshwater Species: From Chemical Mixture to Nanoparticles. *J. Hazard. Mater.* **2023**, *453*, 131402. [[CrossRef](#)]
111. Van Hoeck, A.; Horemans, N.; Van Hees, M.; Nauts, R.; Knapen, D.; Vandenhove, H.; Blust, R. β -Radiation Stress Responses on Growth and Antioxidative Defense System in Plants: A Study with Strontium-90 in *Lemna minor*. *Int. J. Mol. Sci.* **2015**, *16*, 15309–15327. [[CrossRef](#)]

Disclaimer/Publisher’s Note: The statements, opinions and data contained in all publications are solely those of the individual author(s) and contributor(s) and not of MDPI and/or the editor(s). MDPI and/or the editor(s) disclaim responsibility for any injury to people or property resulting from any ideas, methods, instructions or products referred to in the content.